

# Lifting-line theory for an unsteady wing as a singular perturbation problem

By E. C. JAMES

Tetra Tech Incorporated, 630 North Rosemead Boulevard,  
Pasadena, California 91107

(Received 6 November 1972 and in revised form 5 August 1974)

A linearized theory, which treats unsteady motions of a wing of large aspect ratio at variable forward speed in an inviscid incompressible fluid, is developed, using the method of matched asymptotic expansions. The wing geometry and motions are specified; and the time-dependent lift and moment are obtained. Long-time asymptotic behaviour of an initial-value harmonic motion is presented, as are the short-time solutions of a wing starting from rest, with constant acceleration and with impulsive acceleration to constant speed. Some attention is given to flapping flight. Results are presented in quadrature form for a general class of unsteady wing motions.

---

## 1. Introduction

The success of Prandtl's lifting-line theory has prompted many investigations toward a more encompassing theory. The investigations generally concentrate on the development of an integral equation pertinent to the particular lifting-line problem considered. A quite different approach was made by Van Dyke (1963, 1964), who applied matched asymptotic expansions to a large aspect ratio wing at incidence to a steady free stream. He consequently avoided the difficulties of an integral equation, and reduced the problem to one of quadrature, upon obtaining systematic refinements to the two-dimensional results, in terms of an asymptotic series involving the inverse aspect ratio.

This paper develops a linearized theory, which treats unsteady motions of a wing of large aspect ratio at variable forward speeds in an inviscid incompressible fluid. The wing geometry and motions are specified; and the time-dependent lift and moment are obtained. A fundamental assumption is that spanwise perturbations are small on a scale of the flow in planes normal to the span. The method of matched asymptotic expansions is used to obtain Prandtl's acceleration potential  $\Phi$  to one order higher, in inverse aspect ratio, than the strip-theory result. The acceleration potential has been adopted, because it is mathematically more convenient than the velocity potential, which suffers from a discontinuity across the vortex wake.

The solution is obtained by considering a series of simplified problems related to the full problem, in the outer and inner regions. In the outer region, the wing is represented by a line distribution of pressure singularities, whose strengths vary

with time and spanwise location. The lowest-order singularities, occurring on the loaded line, are pressure dipoles with axes parallel to the wing normal. These are followed by pressure quadrupoles and higher-order multipoles. In the inner region, the problem becomes a local investigation of the unsteady motion of a two-dimensional airfoil section. The unsteady, induced velocity on a wing section, owing to the vortex wake, introduces a second-order correction to the acceleration potential in the inner region. The induced velocity is obtained from analysis in the outer region.

Long-time asymptotic behaviour of an initial-value harmonic motion is presented, as are the short-time solutions for a wing of large aspect ratio, starting from rest, with constant acceleration and with impulsive acceleration to constant speed. Results are compared with two-dimensional unsteady airfoil theory, and with three-dimensional steady airfoil theory.

## 2. Formulation

We consider a wing of large aspect ratio, with variable forward speed  $U(t)$ , executing unsteady motions normal to the wing planform. For this investigation, the wing speed is assumed to be small enough to regard the fluid as incompressible. The characteristic Reynolds number, based on wing speed and mean chord length, however, is assumed to be large. The boundary layer along the wing surface is then confined to a narrow adjacent region, and further manifests itself in a thin wake downstream of the trailing edge. We neglect the wing boundary layer, by taking the viscosity to be zero. In the wake, the viscous effects are represented by a planar free vortex sheet, which emanates from the trailing edge, and propagates rearward with stream velocity  $U(t)$ .

Attention is confined to wing geometries of large aspect ratio, where spanwise perturbations are mild compared with those in planes normal to the span. This fundamental assumption is violated at wing tips of 'large' curvature, and gives rise to a local region of non-uniformity. Uniform validity can be achieved by matching the 'wing-tip solution', with the inner and outer solutions. This problem is not treated here. Severe wing-tip difficulties can reasonably be handled, by requiring the loading to fall gradually to zero at the tips over the region of non-uniformity. A quantitative estimate of the extent of this region can be obtained. The results are not valid for 'large' spanwise motions, where other considerations are necessary. (See James 1973.)

At the initial time  $t = 0$ , the wing is at rest in a quiescent fluid, and subsequently achieves a forward speed  $U(t)$  at a later time  $t$ . The wing is sufficiently thin that the transverse displacements of each element of its surface can be described by

$$y = h(x, s, t), \quad |x| \leq c(s)/A \quad (|s| \leq 1, t > 0), \quad (1)$$

in the co-ordinate system fixed to the wing's mean position and where  $y = 0$ ,  $x = \pm c(s)A^{-1}$  ( $|s| \leq 1$ ) gives a symmetric wing planform. The development can readily be extended to include planforms with chordwise and spanwise asymmetries. The arbitrary function  $h(x, s, t)$  is constrained by admitting only wing

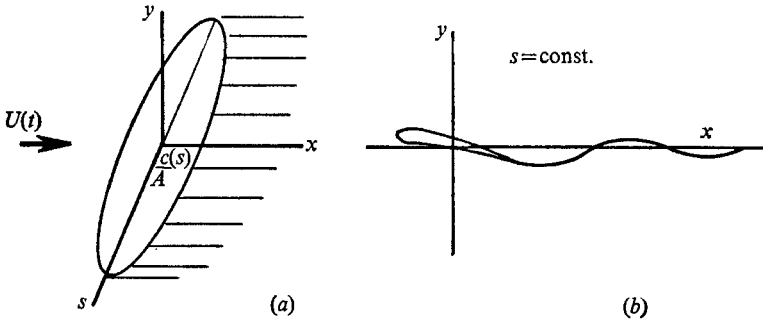


FIGURE 1. (a) Planform of a lifting wing in an unsteady stream. (b) Typical wing section. Mathematically, the wing is represented by the motion of a waving plate of negligible thickness. A singularity at the leading edge of the plate approximates a rounded nose.

displacements that are within the scope of a linearized theory. That is, we admit displacements such that

$$\frac{\partial}{\partial x} h, \quad \frac{\partial}{\partial s} h, \quad U^{-1} \frac{\partial}{\partial t} h \sim o(1).$$

The kinematic boundary condition on the wing specifies the normal component of fluid velocity, which to the linear approximation is

$$v(x, y, s, t) = \left( \frac{\partial}{\partial t} + U(t) \frac{\partial}{\partial x} \right) h(x, s, t) = V_\theta(x, s, \tau) \quad (y = 0^\pm, |x| \leq c(s) A^{-1}, |s| \leq 1). \quad (2)$$

In (2)  $\tau$  is the rectilinear arc length transversed by the wing:

$$\tau(t) = \int_0^t U(t) dt, \quad d\tau = U(t) dt. \quad (3)$$

For positive-definite  $U(t)$ , there is a one-to-one correspondence between  $t$  and  $\tau$ , so that  $t = t(\tau)$  exists. In the sequel, we assume  $U > 0$  for  $t > 0$ , and regard those variables which depend on  $t$  to be dependent variables of  $\tau$  instead.

The linearized Euler equation, relating pressure and velocity, can be written as

$$\left( \frac{\partial}{\partial \tau} + \frac{\partial}{\partial x} \right) \mathbf{q}(\mathbf{x}, \tau) = D\mathbf{q} = \nabla\Phi(\mathbf{x}, \tau) \quad (\mathbf{x} = (x, y, s)), \quad (4)$$

where

$$\Phi(\mathbf{x}, \tau) = \frac{p_\infty - p(\mathbf{x}, t(\tau))}{\rho U(t(\tau))} \quad (5)$$

is a modified form of Prandtl's acceleration potential, and measures the variation of the pressure  $p$  from the static level  $p_\infty$ . The fluid density is  $\rho$ .

$$D = \partial/\partial\tau + \partial/\partial x$$

is a linearized form of the substantial derivative. The perturbation velocity field is  $\mathbf{q}(\mathbf{x}, \tau) = (u, v, w)$  and is divergence and curl free in the field bounded by the wing, the shed vorticity and an encompassing surface at infinity.

By taking the divergence of (4), we see that the acceleration potential satisfies the Laplace equation in the field:

$$\nabla^2\Phi = 0. \tag{6}$$

Across the wing surface,  $\partial\Phi/\partial n$  is continuous, and specified from (4) and (2) to be

$$\partial\Phi(\mathbf{x}, \tau)/\partial y = DV_g(x, s, \tau) \quad (y = 0^\pm, |x| \leq c(s)A^{-1}, |s| \leq 1). \tag{7}$$

From the linearity of  $\Phi$ , the boundary condition (7) and the physical requirement that the pressure be continuous everywhere except across the wing, we can infer that  $\Phi$  is an odd function of  $y$ . Hence

$$\Phi(x, 0, s, \tau) = 0 \quad \text{for } |x| > c(s)A^{-1}. \tag{8}$$

The Kutta–Zhukovskii condition bounds the pressure along a sharp trailing edge. Consequently, it introduces streamwise asymmetry into the problem, since  $\Phi$  may have a singularity at the leading edge. Thus

$$|\Phi(\mathbf{x}, \tau)| < \infty \quad (x = c(s)A^{-1}, y = 0, |s| \leq 1). \tag{9}$$

The boundary-value problem becomes well posed when we further stipulate that the pressure returns to the static level at infinity.

$$\Phi(\mathbf{x}, \tau) \rightarrow 0 \quad \text{as } |\mathbf{x}| \rightarrow \infty. \tag{10}$$

The solution to the linearized boundary-value problem defined by (6)–(10) takes the form of a distribution of pressure dipoles over the wing planform area projected onto the plane  $y = 0$ .

$$\Phi(\mathbf{x}, \tau) = -\frac{1}{4\pi\rho U} \frac{\partial}{\partial y} \int_{-1}^1 \int_{-c_1A^{-1}}^{c_1A^{-1}} \frac{\mathcal{L}(\xi_1, s_1; \tau)}{\mathcal{R}} d\xi_1 ds_1, \tag{11}$$

where  $\mathcal{R} = [(x - \xi_1)^2 + y^2 + (s - s_1)^2]^{\frac{1}{2}}$  and  $c_1 = c(s_1)$ .

$\mathcal{L}(x, s; \tau)$  is the localized pressure jump existing on the wing at a point  $(x, s)$  after the wing has traversed a forward distance  $\tau$ . This can be seen from (11), by fixing a point  $(x, s)$  on the wing, and taking the limit as  $y \rightarrow 0^\pm$ , to give

$$\begin{aligned} \rho U[\Phi(x, 0^+, s; \tau) - \Phi(x, 0^-, s; \tau)] &= p^-(x, s; \tau) - p^+(x, s; \tau) \\ &= \Delta p(x, s; \tau) = \mathcal{L}(x, s; \tau) \quad (|x| < cA^{-1}, |s| \leq 1). \end{aligned} \tag{12}$$

It follows, from (4), that the velocity field is given by

$$\mathbf{q}(\mathbf{x}, \tau) = \int_{x-\tau}^x \left( \mathbf{e}_1 \frac{\partial}{\partial \xi} + \mathbf{e}_2 \frac{\partial}{\partial y} + \mathbf{e}_3 \frac{\partial}{\partial s} \right) \Phi(\xi, y, s, \hat{\tau}(\xi; x)) d\xi, \tag{13}$$

where  $\hat{\tau}(\xi; x) = \tau + \xi - x$  and  $\mathbf{e}_k$  ( $k = 1, 2, 3$ )

are unit base vectors along the  $(x, y, s)$  co-ordinate axes.

### 3. Matched asymptotic expansions: principal results

Formally, we allow the aspect ratio of the wing to become infinite, and deal separately with two simplified asymptotic limits of the problem. These correspond to the two cases of holding the span fixed and letting the chord tend to zero (outer

limit), and of holding the chord fixed and letting the span tend to infinity (inner limit). In the outer limit, the wing collapses to a loaded line. In the inner limit, the ‘section characteristics’ are manifest, where the problem becomes essentially one of two-dimensional unsteady airfoil theory. The outer and inner limits are indeterminate representations of the full problem, since each lacks some essential aspects of the problem: the ‘section characteristics’ in the outer limit, and the interaction of wing sections in the inner limit. A matching of two expansions is needed, to resolve the indeterminacy.

### 3.1. Outer limit

We seek a limiting form of  $\Phi$  which is valid in the outer region where the wing shrinks to a loaded line. This is obtained from the solution to the full problem (11) by letting the chord  $c(s) A^{-1}$  tend to zero. In the limiting process, we expand the kernel function  $\mathcal{R}^{-1}$  in a Taylor series for small  $\xi$ , and integrate term-by-term over the chord. Since

$$\left. \begin{aligned} \mathcal{R}^{-1} &\sim R^{-1} - \xi \frac{\partial}{\partial x} (R^{-1}) + O(\xi^2) \quad (R^2 > \xi^2, \xi^2 \ll 1), \\ R &= [r^2 + (s - s_1)^2]^{\frac{1}{2}}, \quad r^2 = x^2 + y^2, \end{aligned} \right\} \quad (14)$$

we obtain the two-term outer expansion of  $\Phi$ .

$$\Phi(\mathbf{x}; \tau) \sim \frac{-1}{4\pi\rho U} \left\{ \frac{\partial}{\partial y} \int_{-1}^1 \frac{l(s_1; \tau, A)}{R} ds_1 + \frac{\partial^2}{\partial x \partial y} \int_{-1}^1 \frac{m(s_1; \tau, A)}{R} ds_1 + \dots \right\}, \quad (15)$$

where

$$l(s_1; \tau, A) = \int_{-c_1 A^{-1}}^{c_1 A^{-1}} \mathcal{L}(\xi, s_1; \tau) d\xi, \quad m(s_1; \tau, A) = - \int_{-c_1 A^{-1}}^{c_1 A^{-1}} \xi \mathcal{L}(\xi, s_1; \tau) d\xi. \quad (16)$$

In the outer region, the acceleration potential becomes a spanwise distribution of pressure multipoles, the least singular one having dipole character and a strength equal to the section lift. The quadrupole distribution is of strength equal to the first moment of the chordwise lift (positive, nose-up). As the order of the multipoles retained in the outer solution is increased, successively higher moments of section lift are introduced as corresponding distribution strengths. In this way, the outer solution becomes an increasingly refined representation of the full solution. The spanwise lift  $l(s; \tau, A)$  and moment  $m(s; \tau, A)$  each depend parametrically on the aspect ratio  $A$ . Later, they will be expanded in an asymptotic series in the inverse aspect ratio. It is worth noting that (15) can be obtained formally from (11) by specifying

$$\mathcal{L}(\xi, s_1; \tau) = l(s_1; \tau, A) \delta(\xi) + m(s_1; \tau, A) \delta'(\xi) + \dots,$$

where  $\delta(\xi)$  is the Dirac delta function.

We can check that (15) satisfies Laplace’s equation everywhere except on the loaded line. In the outer region, we forego the detailed implications of the wing conditions (7) and (9). We have, however, maintained their broader consequences, in that  $\Phi$  is odd in  $y$  and has streamwise asymmetry. Furthermore, at infinity  $\Phi$  vanishes.

3.2. *Induced velocity*

In this singular perturbation problem, the induced flow on the wing connects the inner and outer limits of the full problem. In the outer region, a simplified approximation of the induced flow will be evaluated. It will be applied as a correction to the specified geometric normal velocity of the wing in the inner region. Within the context of the linearized full problem, the component of the velocity normal to the wing planform on  $y = 0$  is, from (13) and (11),

$$v(x, 0, s; \tau) = \frac{1}{4\pi\rho U} \int_{x-\tau}^x \int_{-1}^1 \int_{-c_1 A^{-1}}^{c_1 A^{-1}} \frac{\mathcal{L}(\xi_1, s_1; \tau + \xi - x)}{[(\xi - \xi_1)^2 + (s - s_1)^2]^{\frac{3}{2}}} d\xi_1 ds_1 d\xi. \quad (17)$$

In the outer limit where the chord tends to zero the leading contribution to the downwash is uniform over the chord. In (17), we assume

$$\mathcal{L}(\xi_1, s_1; \tau + \xi - x) \simeq \delta(\xi_1) l(s_1; \tau + \xi - x, A),$$

and perform the chordwise integration. Making the change of variable  $\tau_1 = x - \xi$ ,  $d\tau_1 = -d\xi$ , integrating by parts with respect to  $\tau_1$  and setting  $x$  to zero gives

$$V_I(s; \tau, A) = \frac{1}{4\pi\rho U} \int_{-1}^1 \frac{1}{(s - s_1)^2} \int_0^\tau \frac{\partial}{\partial(\tau - \tau_1)} l(s_1; \tau - \tau_1, A) \left( \frac{\tau_1^2}{\tau_1^2 + (s - s_1)^2} \right)^{\frac{1}{2}} d\tau_1 ds_1. \quad (18)$$

Additional information about the chordwise distribution of induced flow on the wing can be obtained by including further terms in (17); but, to the order of accuracy of this theory, matching shows such detail to be irrelevant.

The integral over the span must be interpreted as a Hadamard integral, to avoid improper contributions. This has a physical basis, since we must subtract the infinite contribution of the elemental vortex tube that exists at the particular spanwise station  $s$  where the induced velocity is being evaluated. A thorough treatment of Hadamard integrals is contained in Mangler (1951).

Later, for matching purposes, the asymptotic limit of the outer solution, as  $r \rightarrow 0$ , is required. The expansion follows by using the Fourier representation of  $R^{-1}$  in (15), namely

$$R^{-1} = (r^2 + a^2)^{-\frac{1}{2}} = \frac{1}{\pi} \int_{-\infty}^{\infty} K_0(|k|r) \exp(-ika) dk \quad (a = |s - s_1| = 0), \dagger$$

and termwise inverting the ascending-series representation of the modified Bessel function  $K_0$ . Introducing stretched variables

$$\hat{x} = \hat{r} \cos \theta = Ax, \quad \hat{y} = \hat{r} \sin \theta = Ay \quad \text{and} \quad \hat{r} = Ar,$$

the desired result can be expressed as

$$\lim_{\substack{A \rightarrow \infty \\ \hat{r} \text{ fixed}}} \Phi(\mathbf{x}; r) \sim \frac{1}{2\pi\rho U} \left\{ l(s; \tau, A) \frac{\sin \theta}{\hat{r}} + O[l(s; \tau, A) A^{-2} \log A] - Am(s; \tau, A) \frac{\sin 2\theta}{\hat{r}^2} + O[A^{-1}m(s; \tau, A)] + \text{HOT} \right\}. \quad (19)$$

† See Erdélyi *et al.* (1954, p. 49, (40), p. 105, (46)), and extend each equation to the negative real axis.

This result can be verified immediately by taking derivatives (and taking care of the appropriate order-of-magnitude changes) of the standard slender-body source distribution expansion. (See e.g. Ashley & Landahl 1965.) In the limit  $r \rightarrow 0$ , the distributions of three-dimensional dipoles and quadrupoles reduce to their two-dimensional counterparts plus regular terms (denoted by order symbols). It is significant that the regular terms are two orders of magnitude smaller in inverse aspect ratio than their respective antecedents. ‘HOT’ stands for the neglected higher-order multipole terms of the outer expansion. According to the principle of minimum singularity (Van Dyke 1964, p. 53), the correction introduced by retaining a higher-order singularity should be small on a scale of the primary influence of an antecedent lower-order singularity. On this basis, the quadrupole term provides a small correction to the leading order of the dipole contribution. For our problem, this principle gives the correct ordering. Equation (19) represents the two-term inner expansion of the two-term outer expansion of  $\Phi$ .

### 3.3. Inner limit

The details of the flow close to the wing are investigated by stretching the co-ordinates normal to the span, so that the two-dimensional character of the flow is emphasized. If we choose

$$\hat{x} = Ax, \quad \hat{y} = Ay, \quad \hat{s} = s, \quad \hat{t} = At, \tag{20}$$

for inner variables, the relevant length scale becomes the semichord  $c(s)$ . Magnifying time  $t$  is mathematically convenient, and does not alter the form of solution, since time enters as a parameter. However, we must later return to the proper time scale for physical interpretation. As a consequence of (20), the near field is characterized by variations of the physical quantities having

$$\frac{\partial}{\partial \hat{x}}, \quad \frac{\partial}{\partial \hat{y}}, \quad \frac{\partial}{\partial \hat{t}} \sim O(A) \quad \text{and} \quad \frac{\partial}{\partial \hat{s}} \sim O(1).$$

The wing displacement function  $h(x, s, t)$  and its associated normal velocity  $V_g$  (see (1)), when referred to inner variables, are

$$\left. \begin{aligned} \hat{y} &= \hat{h}(\hat{x}, \hat{s}, \hat{t}) = Ah(\hat{x}A^{-1}, s, \hat{t}A^{-1}) \quad (|\hat{x}| \leq c, |s| \leq 1), \\ \hat{V}_g(\hat{x}, s, \hat{t}) &= \left[ \frac{\partial}{\partial \hat{t}} + U \frac{\partial}{\partial \hat{x}} \right] \hat{h}(\hat{x}, s, \hat{t}) = V_g(x, s, \tau) \quad (|x| \leq c, |s| \leq 1), \\ \hat{V}_g(\hat{x}, s, \hat{t}) &= \frac{1}{2}b_0(s, \hat{t}(\hat{\tau})) + \sum_{j=1}^{\infty} b_j(s, \hat{t}(\hat{\tau})) \cos j\theta \quad (\hat{x} = c \cos \theta), \end{aligned} \right\} \tag{21}$$

where the Fourier coefficients are

$$\left. \begin{aligned} b_n(s, \hat{t}(\hat{\tau})) &= \frac{2}{\pi} \int_0^\pi \hat{V}_g(\hat{x}, s, \hat{t}) \cos n\theta d\theta \quad (n = 0, 1, 2, \dots), \\ \hat{\tau} &= A\tau = A \int_0^{\hat{t}A^{-1}} U(t_1) dt_1. \end{aligned} \right\} \tag{22}$$

It is noteworthy that the geometrically specified normal velocity  $\hat{V}_g$  of the wing section appears independent of the aspect ratio. As a consequence, we tentatively expand the normal velocity  $\hat{v}(\hat{x}, \hat{y}; s, \hat{t}, A)$  on the wing as

$$\left. \begin{aligned} \hat{v}(\hat{x}, \hat{y}; s, \hat{t}, A) &\sim \hat{v}_1(\hat{x}, \hat{y}; s, \hat{t}) + A^{-1}\hat{v}_2(\hat{x}, \hat{y}; s, \hat{t}) + \dots \\ & \quad (|\hat{x}| \leq c, |s| \leq 1, \hat{y} = 0 \pm, A \rightarrow \infty) \end{aligned} \right\} \quad (23)$$

$$\sim \hat{V}_g(\hat{x}, s, \hat{t}) - \hat{V}_I(s, \hat{t}, A),$$

$$\hat{v}_1(\hat{x}, 0; s, \hat{t}) = \hat{V}_g(\hat{x}, s, \hat{t}), \quad \hat{v}_2(\hat{x}, 0; s, \hat{t}) = - \lim_{A \rightarrow \infty} A \hat{V}_I(s, \hat{t}, A), \quad (24)$$

$$\left. \begin{aligned} \hat{V}_I(s, \hat{t}, A) &= V_I(s, \hat{t}A^{-1}, A), \\ \hat{V}_I(s, \hat{t}, A) &= \frac{1}{4\pi\rho U} \int_{-1}^1 \frac{1}{(s-s_1)^2} \int_0^{\hat{t}} \frac{\partial}{\partial(\hat{t}-\hat{t}_1)} l\left(s_1, \frac{\hat{t}-\hat{t}_1}{A}, A\right) \left[ \frac{\tau_1^2}{\tau_1^2 + A^2(s-s_1)^2} \right]^{\frac{1}{2}} d\hat{t}_1 ds_1. \end{aligned} \right\} \quad (25)$$

Thus, the wing is impervious to the induced flow, which presumably makes a small correction to the velocity  $\hat{V}_g$ . The correction velocity  $\hat{v}_2(\hat{x}, 0; s, \hat{t})$  is uniform over the chord, the appropriate ‘Prandtl-order’ result for a wing of large aspect ratio. Higher-order refinement will obviously bring in chordwise variation as well.

In the inner region, the acceleration potential  $\Phi(\mathbf{x}; \tau)$  is expressed as  $\Phi(\hat{x}; \tau) = \phi(\hat{x}, \hat{y}; s, \hat{t}, A)$ , where  $\phi$  depends parametrically on  $s$  and  $\tau$ , and may be expanded in an asymptotic series in the inverse aspect ratio:

$$\phi(\hat{x}, \hat{y}; s, \hat{t}, A) \sim A^{-1}\phi_1(\hat{x}, \hat{y}; s, \hat{t}) + A^{-2}\phi_2(\hat{x}, \hat{y}, s, \hat{t}) + \dots \quad (A \rightarrow \infty). \quad (26)$$

It follows from (23) and the wing boundary condition (7), expressed in terms of inner variables, that  $\phi(\hat{x}, \hat{y}; s, \hat{t}, A) \sim O(A^{-1})$ . The order of the second term in the expansion (26) must be regarded as a conjecture at this stage. Using (20), (23) and (26), the full problem becomes

$$\left[ \frac{\partial^2}{\partial \hat{x}^2} + \frac{\partial^2}{\partial \hat{y}^2} \right] \phi_k(\hat{x}, \hat{y}; s, \hat{t}) = 0, \quad (27)$$

$$\frac{\partial}{\partial \hat{y}} \phi_k(\hat{x}, \hat{y}; s, \hat{t}) = \left[ \frac{\partial}{\partial \hat{t}} + \frac{\partial}{\partial \hat{x}} \right] \hat{v}_k(\hat{x}, \hat{y}; s, \hat{t}) \quad (|\hat{x}| \leq c, |s| \leq 1, \hat{y} = 0 \pm), \quad (28)$$

$$\phi_k(\hat{x}, \hat{y}; s, \hat{t}) = 0 \quad (|\hat{x}| > c, \hat{y} = 0), \quad (29)$$

$$|\phi_k(\hat{x}, \hat{y}; s, \hat{t})| < \infty \quad (\hat{x} = c, \hat{y} = 0, |s| \leq 1), \quad (30)$$

$$\phi_k(\hat{x}, \hat{y}; s, \hat{t}) \rightarrow 0 \quad \text{as} \quad \hat{t} = (\hat{x}^2 + \hat{y}^2)^{\frac{1}{2}} \rightarrow \infty, \quad (31)$$

where  $k = 1, 2$ .

Because we have introduced stretched variables, the behaviour of  $\phi$  at infinity is lost. It is sufficient (at least for the first two terms of the asymptotic expansion of  $\phi$ ) to assert that  $\phi$  vanishes at infinity. An arbitrary function of  $s$  and  $\tau$  is ruled out, since  $\phi$  is an odd function of  $y$ . Unbounded behaviour proves to be unmatchable. It can be seen from (27)–(31) that, if the correction term to the strip-theory result is  $O(A^{-2})$ , the boundary-value problems for  $\phi_1$  and  $\phi_2$  are identical.



The solution of this classical problem can be found in the literature. (See e.g. Wu 1971*a*.)

$$\phi_k(\hat{x}, \hat{y}; s, \hat{t}) = \text{Re} \left\{ \frac{1}{\pi i} \left[ \frac{\hat{z}-c}{\hat{z}+c} \right]^{\frac{1}{2}} \int_{-c}^c \frac{[c+\xi]^{\frac{1}{2}} g_k(\xi; s, \hat{t})}{(c-\xi)} d\xi \right\}, \tag{32}$$

$$\hat{z} = \hat{x} + i\hat{y}, \quad \hat{x} = \hat{r} \cos \theta, \quad \hat{y} = \hat{r} \sin \theta, \quad \hat{r} = (\hat{x}^2 + \hat{y}^2)^{\frac{1}{2}},$$

$$g_k(\hat{x}; s, \hat{t}) = - \left[ \frac{\partial}{\partial \hat{t}} + \frac{\partial}{\partial \hat{x}} \right] \int_{-c}^{\hat{x}} \hat{v}_k(\xi, 0; s, \hat{t}) d\xi + A_k(s, \hat{t}) \quad (|\hat{x}| \leq c), \tag{33a}$$

$$A_k(s, \hat{t}) = \frac{1}{\pi} \int_{-c}^c (c^2 - \xi^2)^{-\frac{1}{2}} \left( \frac{\partial}{\partial \hat{t}} + \frac{\partial}{\partial \xi} \right) \int_{-c}^{\xi} \hat{v}_k(\hat{x}, 0; s, \hat{t}) d\hat{x} d\xi + \frac{1}{2} a_k(s, \tau), \tag{33b}$$

$$a_k(s, \hat{t}) = \frac{2}{\pi} \int_{-c}^c \frac{(\xi/c) \hat{v}_k(\xi, 0; s, \tau)}{(c^2 - \xi^2)^{\frac{1}{2}}} d\xi - \frac{2}{\pi c} \int_{-c}^c \frac{(1 + \xi/c)}{(c^2 - \xi^2)^{\frac{1}{2}}} \int_0^{\hat{t}} H \left( \frac{\hat{t} - \hat{t}_1}{c} \right) \hat{v}_k(\xi, 0; s, \hat{t}_1) d\hat{t}_1 d\xi, \tag{33c}$$

$$H(\hat{t}) = \frac{1}{2\pi i} \int_{\epsilon - i\infty}^{\epsilon + i\infty} \exp(\zeta \hat{t}) \left[ \frac{K_1(\zeta)}{K_0(\zeta) + K_1(\zeta)} \right] d\zeta \quad (\epsilon > 0). \tag{33d}$$

$K_0$  and  $K_1$  are modified Bessel functions. In the solution (32),  $[(\hat{z}-c)/(\hat{z}+c)]^{\frac{1}{2}}$  has a branch cut from  $\hat{z} = -c$  to  $\hat{z} = c$ , and tends to unity as  $|\hat{z}| \rightarrow \infty$ . Taking the limit as  $|\hat{z}| \rightarrow \infty$  of  $\phi_k(\hat{x}, \hat{y}; s, \hat{t})$  in (32) results in the outer expansion of the inner acceleration potentials.

$$\phi_k(\hat{x}, \hat{y}; s, \hat{t}) \sim \lambda_k(s, \hat{t}) \frac{\sin \theta}{\hat{r}} + \mu_k(s, \hat{t}) \frac{\sin 2\theta}{\hat{r}^2} + O(\hat{r}^{-3}) \quad (\hat{r} \rightarrow \infty), \tag{34}$$

$$\lambda_k(s, \hat{t}) = \frac{1}{\pi} \int_{-c}^c \left[ \frac{1 + \xi/c}{1 - \xi/c} \right]^{\frac{1}{2}} g_k(\xi, s, \hat{t}) d\xi, \tag{35}$$

$$\mu_k(s, \hat{t}) = -\frac{c}{\pi} \int_{-c}^c (1 - \xi/c) \left[ \frac{1 + \xi/c}{1 - \xi/c} \right]^{\frac{1}{2}} g_k(\xi, s, \hat{t}) d\xi. \tag{36}$$

Substituting (34) into (26), and using (20) to express the result in physical variables, gives, for the two-term outer expansion of the two-term inner expansion,

$$\left( \begin{array}{c} \text{2-term outer} \\ \text{of} \\ \text{2-term inner} \end{array} \right) \Phi(\mathbf{x}, \tau) \sim A^{-1} \left[ \frac{\lambda_1(s, \hat{t})}{A} + \frac{\lambda_2(s, \hat{t})}{A^2} \right] \frac{\sin \theta}{r} + A^{-1} \left[ \frac{\mu_1}{A^2} + \frac{\mu_2}{A^3} \right] \frac{\sin 2\theta}{r^2} \quad (A \rightarrow \infty, r \text{ fixed}). \tag{37}$$

Provided the wing does not have abrupt spanwise geometric variations, this expression will be uniformly valid in  $s$ . As mentioned previously, special attention must be given to ‘blunt’ wing tips.

From (19) we rewrite the two-term inner expansion of the two-term outer expansion as

$$\left( \begin{array}{c} \text{2-term inner} \\ \text{of} \\ \text{2-term outer} \end{array} \right) \Phi(x, \tau) \sim \frac{1}{2\pi\rho U} \left\{ l(s, \tau; A) \frac{\sin \theta}{\hat{r}} + O[l(s, \tau; A) A^{-2} \log A] - Am(s, \tau; A) \frac{\sin 2\theta}{\hat{r}^2} + O[A^{-1}m(s, \tau; A)] \right\} \quad (A \rightarrow \infty, r \text{ fixed}).$$

Inner potential	Outer potential	Matching result
$A^{-1} \left[ \frac{\lambda_1(s, \hat{\tau})}{A} \right] \frac{\sin \theta}{r}$	$A^{-1} \left[ \frac{l(s, \tau, A)}{2\pi\rho U} \right] \frac{\sin \theta}{r}$	$l(s, \tau, A) = 2\pi\rho U \lambda_1(s, \hat{\tau}) A^{-1}$
$A^{-1} \left[ \frac{\lambda_1}{A} \right] \frac{\sin \theta}{r}$	$A^{-1} \left[ \frac{l(s, \tau, A)}{2\pi\rho U} \right] \frac{\sin \theta}{r}$	
$+ \frac{1}{A} \left[ \frac{\mu_1}{A^2} \right] \frac{\sin 2\theta}{r^2}$	$- \frac{m(s, \tau, A)}{2\pi\rho U} \frac{\sin 2\theta}{r^2}$	$m(s, \tau, A) = -2\pi\rho U \mu_1(s, \hat{\tau}) A^{-2}$
$A^{-1} \left[ \frac{\lambda_1 + \lambda_2}{A + A^2} \right] \frac{\sin \theta}{r}$	$A^{-1} \left[ \frac{l(s, \tau, A)}{2\pi\rho U} \right] \frac{\sin \theta}{r}$	$l(s, \tau, A) = 2\pi\rho U \left( \frac{\lambda_1}{A} + \frac{\lambda_2}{A^2} \right)$
$A^{-1} \left[ \frac{\lambda_1 + \lambda_2}{A + A^2} \right] \frac{\sin \theta}{r}$	$A^{-1} \left[ \frac{l(s, \tau, A)}{2\pi\rho U} \right] \frac{\sin \theta}{r}$	$l(s, \tau, A) = 2\pi\rho U \left( \frac{\lambda_1}{A} + \frac{\lambda_2}{A^2} \right)$
$+ A^{-1} \left[ \frac{\mu_1 + \mu_2}{A^2 + A^3} \right] \frac{\sin 2\theta}{r^2}$	$- \frac{m(s, \tau, A)}{2\pi\rho U} \frac{\sin 2\theta}{r^2}$	$m(s, \tau, A) = -2\pi\rho U \left( \frac{\mu_1}{A^2} + \frac{\mu_2}{A^3} \right)$

TABLE 1

The inner and outer expansions must be matched, using the same spatial variables.  $\tau$  and  $\hat{\tau}$  are free parameters with respect to the matching, and are not influenced by the limit  $A \rightarrow \infty$ . The matching proceeds with (37) and (19), even though we use  $\hat{\tau}$  in one and  $\tau$  in the other. As mentioned previously, however,  $\hat{\tau}$  must be replaced with  $A\tau$  for the proper physical interpretation of the final results.

Table 1 presents the results of a step-by-step application of the asymptotic matching principle (Van Dyke 1964). The  $m$ -term inner expansion of (the  $n$ -term outer expansion) equals the  $n$ -term outer expansion of (the  $m$ -term inner expansion). The unmatchable regular terms of the outer solution are  $O(A^{-3} \log A)$ , in terms of the inner variables, and may be disregarded. They will match, however, with the third-order inner acceleration potential  $\phi_3$ , which satisfies a two-dimensional Poisson equation and has  $\hat{\tau} \sin \theta$  behaviour as  $\hat{\tau} \rightarrow \infty$ . It is simple to justify the validity of the assumed expansion of the inner acceleration potential (26) since  $l(s, \tau; A) \sim O(A^{-1})$ . The quantity  $A\hat{V}_I(s, \hat{\tau}; A)$  is independent of the aspect ratio as  $A \rightarrow \infty$ , so that the induced flow is indeed a small correction to  $\hat{V}_g$ . (See (23)–(25).) From (24), (25) and table 1, we define  $\hat{V}_I(s, \hat{\tau})$  as

$$\hat{v}_2(x, 0; s, \hat{\tau}) = -\hat{V}_I(s, \hat{\tau}) \quad (|\hat{x}| \leq c, |s| \leq 1),$$

$$\hat{V}_I(s, \hat{\tau}) = \frac{1}{2} \int_{-1}^1 \frac{1}{(s-s_1)^2} \int_0^{\hat{\tau}} \frac{\partial}{\partial(\hat{\tau}-\hat{\tau}_1)} \lambda_1(s_1, \hat{\tau}-\hat{\tau}_1) \left[ \frac{\hat{\tau}_1^2}{\hat{\tau}_1^2 + A^2(s-s_1)^2} \right]^{\frac{1}{2}} d\hat{\tau}_1 ds_1. \quad (38)$$

In table 1, the second level of matching displays the strip-theory results for the lift and moment. They can be expressed in terms of the Fourier coefficients of  $\hat{V}_g$  given in (21). Using (33) in (35) and (36), and performing one integration by

parts, allows one to introduce the Fourier coefficients in each term. The corresponding two-dimensional expressions for lift and moment, developed by Wu (1971*a*), are recovered.

$$\lambda_1(s, \hat{\tau}) = \frac{1}{2}c \left\{ a_1(s, \hat{\tau}) - b_1(s, \hat{\tau}) - \frac{1}{2}c \frac{\partial}{\partial \hat{\tau}} [b_0(s, \hat{\tau}) - b_2(s, \hat{\tau})] \right\}, \tag{39}$$

$$\mu_1(s, \hat{\tau}) = \frac{1}{4}c^2 \left\{ a_1(s, \hat{\tau}) + b_2(s, \hat{\tau}) + \frac{1}{4}c \frac{\partial}{\partial \hat{\tau}} [b_1(s, \hat{\tau}) - b_3(s, \hat{\tau})] \right\}, \tag{40}$$

$$a_1(s, \tau) = b_1(s, \hat{\tau}) - \frac{1}{c} \int_0^{\hat{\tau}} H((\hat{\tau} - \hat{\tau}_1)/c) [b_0(s, \hat{\tau}_1) + b_1(s, \hat{\tau}_1)] d\hat{\tau}_1. \tag{41}$$

$\lambda_2$  and  $\mu_2$  can be written down by inspection of (39)–(41). In fact,  $\lambda_2$  and  $\mu_2$  are equal to  $\lambda_1$  and  $\mu_1$ , respectively, when  $b_0$  is replaced by  $-2\hat{V}_T(s, \hat{\tau})$  and  $b_1, b_2$  and  $b_3$  are set to zero. Hence,

$$\lambda_2(s, \hat{\tau}) = \frac{1}{2}c \left[ \frac{2}{c} \int_0^{\hat{\tau}} H((\hat{\tau} - \hat{\tau}_1)/c) \hat{V}_T(s, \hat{\tau}) d\hat{\tau}_1 + c \frac{\partial}{\partial \hat{\tau}} \hat{V}_T(s, \hat{\tau}) \right], \tag{42}$$

$$\mu_2(s, \hat{\tau}) = \frac{1}{4}c^2 \left[ \frac{2}{c} \int_0^{\hat{\tau}} H((\hat{\tau} - \hat{\tau}_1)/c) \hat{V}_T(s, \hat{\tau}) d\hat{\tau}_1 \right]. \tag{43}$$

#### 4. Matched asymptotic expansions: results for short- and long-time limits

The principal results of this investigation are contained in (38)–(43). In the sequel we shall develop results for short- and long-time limits for various wing motions. The particular cases of interest are readily investigated in the Laplace transform plane, where the transform is taken with respect to the unstretched ‘time’  $\tau$ . Since  $\hat{\tau} = A\tau$ , the transformed equations (39)–(43) depend on the aspect ratio.

$$\left. \begin{aligned} \tilde{\lambda}_1(s, p; A) &= \int_0^\infty \exp(-p\tau) \lambda_1(s, \tau A) d\tau = A^{-1} \int_0^\infty \exp[-(pA^{-1})\hat{\tau}] \lambda_1(s, \hat{\tau}) d\hat{\tau} \\ &= A^{-1} \tilde{\lambda}_1(s, pA^{-1}) \\ &= \frac{1}{2}cA^{-1} \{ \tilde{a}_1(s, pA^{-1}) - \tilde{b}_1(s, pA^{-1}) - \frac{1}{2}cpA^{-1} [\tilde{b}_1(s, pA^{-1}) - \tilde{b}_2(s, pA^{-1})] \}, \end{aligned} \right\} \tag{44}$$

$$\tilde{\mu}_1(s, p; A) = \frac{1}{4}c^2A^{-1} \{ \tilde{a}_1(s, pA^{-1}) + \tilde{b}_2(s, pA^{-1}) + \frac{1}{4}cpA^{-1} [\tilde{b}_1(s, pA^{-1}) - \tilde{b}_3(s, pA^{-1})] \}, \tag{45}$$

$$\tilde{a}_1(s, pA^{-1}) = \tilde{b}_1(s, pA^{-1}) - \tilde{H}(pcA^{-1}) [\tilde{b}_0(s, pA^{-1}) + \tilde{b}_1(s, pA^{-1})], \tag{46}$$

$$\tilde{H}(cpA^{-1}) = K_1(cpA^{-1}) [K_0(cpA^{-1}) + K_1(cpA^{-1})]^{-1}, \tag{47}$$

$$\tilde{\lambda}_2(s, p; A) = cA^{-1} [\tilde{H}(cpA^{-1}) + \frac{1}{2}cpA^{-1}] \tilde{V}_1(s, pA^{-1}), \tag{48}$$

$$\tilde{\mu}_2(s, p; A) = \frac{1}{2}c^2A^{-1} \tilde{H}(cpA^{-1}) \tilde{V}_1(s, pA^{-1}), \tag{49}$$

$$\tilde{V}_1(s, pA^{-1}) = \frac{1}{2} \int_{-1}^1 \frac{\tilde{G}(p|s-s_1|) \tilde{\lambda}_1(s_1, pA^{-1})}{(s-s_1)^2} ds_1, \tag{50}$$

$$\tilde{G}(p|s-s_1|) = p|s-s_1| \{ \frac{1}{2}\pi [\mathbf{H}_1(p|s-s_1|) - Y_1(p|s-s_1|)] - 1 \}. \tag{51}$$

$K_0, K_1$  are modified Bessel functions,  $Y_1$  is a Bessel function of the second kind, and  $\mathbf{H}_1$  is a Struve function.

The long- and short-time limiting forms for the lift and moment are obtained by taking the limits of (44)–(51) as  $|p| \rightarrow 0$  and  $p \rightarrow \infty$ , respectively, and inverting. The following series expansions of  $\tilde{H}$  and  $\tilde{G}$ , developed in Abramowitz & Stegun (1964), will be useful:

$$\begin{aligned} \lim_{\zeta \rightarrow 0} \tilde{H}(\zeta) &\sim 1 + (\gamma + \log 2)\zeta + \zeta \log \zeta + O(\zeta^2 \log^2 \zeta), \\ \lim_{\zeta_1 \rightarrow 0} \tilde{G}(\zeta_1) &\sim 1 - \zeta_1 + \frac{1}{2}(\frac{1}{2} + \log 2 - \gamma)\zeta_1^2 - \frac{1}{2}\zeta_1^2 \log \zeta_1 + O(\zeta_1^3), \\ \lim_{\zeta \rightarrow \infty} \tilde{H}(\zeta) &\sim \frac{1}{2}(1 + \frac{1}{4}\zeta^{-1}) + O(\zeta^{-2}), \\ \lim_{\zeta_1 \rightarrow \infty} \tilde{G}(\zeta_1) &\sim \zeta_1^{-1} - 3\zeta_1^{-3} + O(\zeta_1^{-5}). \end{aligned}$$

Euler’s constant  $\gamma = 0.57721$ .  $\tilde{H}$  and  $\tilde{G}$  are each defined with a branch cut along the negative real axis. The differences in  $\tilde{H}$  and in  $\tilde{G}$  as we approach the branch cut from the bottom and the top are

$$\begin{aligned} [\tilde{H}^-(\zeta) - \tilde{H}^+(\zeta)] &\sim -2\pi i \zeta + O(\zeta^2 \log \zeta) \quad (\zeta \ll 1, \text{ real and negative}), \\ [\tilde{G}^-(\zeta_1) - \tilde{G}^+(\zeta_1)] &\sim \pi i \zeta_1^2 + O(\zeta_1^3) \quad (\zeta_1 \ll 1, \text{ real and negative}). \end{aligned}$$

4.1. *Impulsive acceleration to constant speed*

In this simple case, the wing is at constant angle of incidence  $-\alpha$  to the direction in which a quiescent fluid is impulsively accelerated from rest to a constant speed  $U$ . The situation is formally equivalent to a step-function change in angle of attack at constant forward speed. The non-vanishing coefficient for  $\hat{V}_g$  is

$$b_0(s, \hat{t}) = -2U\alpha \quad (\hat{t} > 0),$$

implying  $\tilde{b}_0(s, pA^{-1}) = -2U\alpha A/p$ . Equations (44)–(51) become

$$\tilde{\lambda}_1(s, p; A) = U\alpha c \tilde{H}(pcA^{-1})/p, \tag{52}$$

$$\tilde{\mu}_1(s, p; A) = \frac{1}{2}U\alpha c^2 \tilde{H}(pcA^{-1})/p, \tag{53}$$

$$\tilde{\lambda}_2(s, p; A) = \frac{1}{2}U\alpha c [\tilde{H}(cpA^{-1}) + \frac{1}{2}cpA^{-1}] \int_{-1}^1 \frac{c_1 \tilde{H}(c_1 pA^{-1}) \tilde{G}(p|s-s_1|)}{p(s-s_1)^2} ds_1, \tag{54}$$

$$\tilde{\mu}_2(s, p; A) = \frac{1}{4}U\alpha c^2 \tilde{H}\left(\frac{cp}{A}\right) \int_{-1}^1 \frac{c_1 \tilde{H}(c_1 pA^{-1}) \tilde{G}(p|s-s_1|)}{p(s-s_1)^2} ds_1. \tag{55}$$

The Laplace inversion formula is

$$B(\tau) = \frac{1}{2\pi i} \int_{\epsilon-i\infty}^{\epsilon+i\infty} \exp(p\tau) \tilde{B}(p) dp \quad (\epsilon > 0);$$

and in our special case  $\tilde{B}(p)$  has a branch cut along the negative real axis and a pole at the origin. The path of integration can be deformed into a small circle (counter-clockwise) about the origin, and a contour  $C$  circumventing the negative real axis counter-clockwise. The contour integral about the origin can be evaluated directly by the residue theorem, whereas the contour integral  $C$  can be evaluated

for large  $\tau$  by expanding the integrand for small  $|p|$  and applying Watson's lemma. For  $\tau \gg cA^{-1}$ , we obtain

$$\lambda_1(s, A\tau) = U\alpha c\{1 - cA^{-1}/\tau + O[(cA^{-1}/\tau)^2]\}, \tag{56}$$

$$\mu_1(s, A\tau) = \frac{1}{2}U\alpha c^2\{1 - cA^{-1}/\tau + O[(cA^{-1}/\tau)^2]\}, \tag{57}$$

$$\lambda_2(s, A\tau) = \frac{1}{2}U\alpha c \left\{ \oint_{-1}^1 \frac{c(s_1)}{(s-s_1)^2} ds_1 - cA^{-1}/\tau \oint_{-1}^1 \frac{[1+c(s_1)/c(s)]}{(s-s_1)^2} ds_1 + O[(cA^{-1}/\tau)^2] \right\}, \tag{58}$$

$$\mu_2(s, A\tau) = \frac{1}{2}c\lambda_2(s, \tau A). \tag{59}$$

In (56)–(59), setting  $\tau = \infty$  recovers the steady-state limit. Integrating the Hadamard integral by parts gives a Cauchy principal-value integral. The steady lift and moments per unit span are, therefore,

$$l(s, \infty; A) \simeq 2\pi\rho U^2\alpha cA^{-1} \left\{ 1 - \frac{1}{2} \oint_{-1}^1 \frac{c(s_1)A^{-1}}{(s-s_1)} ds_1 \right\}, \tag{60}$$

$$m(s, \infty; A) \simeq -\frac{1}{2}cA^{-1}l(s, \infty; A). \tag{61}$$

Equation (60) is identical to Van Dyke's (1963, 1964) result.

For small  $\tau$ , the lift and moment are found directly from (52)–(55) by expanding for large  $p$  and inverting:

$$\lambda_1(s, \tau A) \sim \frac{1}{2}U\alpha c\{1 + \frac{1}{4}\tau/(cA^{-1}) + O\{[\tau/(cA^{-1})]^2\}\},$$

$$\mu_1(s, \tau A) = \frac{1}{2}c\lambda_1(s, \tau A), \quad \tau \ll cA^{-1},$$

$$\lambda_2(s, \tau A) \sim \frac{1}{8}U\alpha(cA^{-1}) \left\{ c \oint_{-1}^1 \frac{c_1 ds_1}{|s-s_1|^3} + \tau/(cA^{-1}) \oint_{-1}^1 \frac{c(c_1 + \frac{1}{4}c)}{|s-s_1|^3} ds_1 + O\{\tau/(cA^{-1})^2\} \right\},$$

$$\mu_2(s, \tau A) \sim \frac{1}{16}U\alpha(c^2A^{-1}) \left\{ \tau/(cA^{-1}) \oint_{-1}^1 \frac{cc_1 ds_1}{|s-s_1|^3} + O\{\tau/(cA^{-1})^2\} \right\}.$$

Immediately after the initial instant, the lift and moment per unit span are

$$l(s, 0; A) \simeq \pi\rho U^2\alpha cA^{-1} \left\{ 1 + \frac{c}{A^2} \oint_{-1}^1 \frac{c(s_1)}{|s-s_1|^3} ds_1 + O(A^{-2}) \right\}, \tag{62}$$

$$m(s, 0; A) \simeq -\frac{1}{2}\pi\rho U^2\alpha c^2A^{-2}\{1 + O(A^{-2})\}. \tag{63}$$

The 'small' three-dimensional correction term of the initial lift expression is due to the impulsive pressure induced on each wing section by the starting vortex wake. Since this term is  $O(A^{-3})$  in the lift, the starting lift is essentially the two-dimensional value.

#### 4.2. Case of constant acceleration $\dot{U}$

Only the initial motion is of interest here. We set  $U = \dot{U}t$ ; and during the acceleration the wing traverses a distance  $\tau = \frac{1}{2}\dot{U}t^2$  at a constant angle of incidence  $-\alpha$ . The non-vanishing Fourier coefficient is

$$b_0(s, \hat{t}) = -2U(t\hat{t})\alpha = -2\alpha(2\dot{U}A^{-1})^{\frac{1}{2}}(\hat{t})^{\frac{1}{2}}.$$

The resulting lift and moment per unit span are found to be

$$l(s, \tau; A) \sim \pi\rho\dot{U}(c^2A^{-2})\{1 + O(t^2, A^{-2})\} \quad (t \ll 1, A \gg 1),$$

$$m(s, \tau; A) \sim \pi\rho\dot{U}\alpha(c^3A^{-3})\{O(t^2, A^{-2})\} \quad (t \ll 1, A \gg 1).$$

The lift immediately attains a constant value, which varies directly with the acceleration  $\dot{U}$ , whereas the moment about the midchord is zero. The three-dimensionality enters as a higher-order effect in this small-time solution, again indicating that the wing initially responds as if its span is infinite. Since the centre of pressure is at the midchord, the initial lift is due to the impulsive pressure generated by the starting motion.

4.3. Simple harmonic motion at constant speed  $U$

We write the displacement of a thin wing section as

$$\hat{y} = \hat{h}(\hat{x}, s, \hat{t}) = \{ \frac{1}{2} \xi_0(s) + [\xi_1(s) + j\xi_2(s)] \hat{x} \} \exp(j\omega A^{-1} \hat{t}) \quad (|\hat{x}| < c). \tag{64}$$

$\frac{1}{2} \xi_0$  is the sectional amplitude of heaving motion, and  $|\xi_1 + j\xi_2|$  is the sectional amplitude of the pitching about the midchord. The pitching leads the heaving by the phase angle  $\alpha_\rho = tg^{-1}(\xi_2/\xi_1)$ . The specified normal velocity of the wing section is

$$\left. \begin{aligned} \hat{V}_1(\hat{x}, 0, s, \hat{t}) &= \{ \frac{1}{2} b_0(s) + b_1(s) \hat{x}/c \} \exp(j\omega A^{-1} \hat{t}) \quad (|\hat{x}| < c), \\ b_0(s, \hat{t}) &= b_0(s) \exp(j\omega U^{-1} \hat{t} A^{-1}) = \{ j\omega A^{-1} \xi_0(s) + 2U(\xi_1(s) + j\xi_2(s)) \} \exp(j\omega U^{-1} \hat{t} A^{-1}), \\ b_1(s_1 \hat{t}) &= b_1(s) \exp(j\omega U^{-1} \hat{t} A^{-1}) = \{ j\omega A^{-1} c(s) [\xi_1(s) + j\xi_2(s)] \} \exp(j\omega U^{-1} \hat{t} A^{-1}), \end{aligned} \right\} \tag{65}$$

$$\tilde{b}_0(s, pA^{-1}) = Ab_0(s)[p - j\omega/U]^{-1}, \quad \tilde{b}_1(s, pA^{-1}) = Ab_1(s)[p - j\omega/U]^{-1}. \tag{66}, \tag{67}$$

Substituting (66), (67) into (44)–(51) gives

$$\tilde{\lambda}_1(s, p; A) = -\frac{1}{2}c \left\{ \frac{\tilde{H}(pcA^{-1})[b_0(s) + b_1(s)] + \frac{1}{2}(cpA^{-1})b_0(s)}{(p - j\omega/U)} \right\}, \tag{68}$$

$$\tilde{\mu}_1(s, p; A) = \frac{1}{4}c^2 \left\{ \frac{[1 + \frac{1}{4}(cpA^{-1})]b_1(s) - \tilde{H}(pcA^{-1})[b_0(s) + b_1(s)]}{(p - j\omega/U)} \right\}, \tag{69}$$

$$\begin{aligned} \tilde{\lambda}_2(s, p; A) &= -\frac{1}{4}c[\tilde{H}(cpA^{-1}) + \frac{1}{2}cpA^{-1}] \\ &\quad \times \int_{-1}^1 \frac{c_1 \tilde{G}(p|s - s_1|) [\tilde{H}(c_1 pA^{-1})(b_0(s) + b_1(s)) + \frac{1}{2}c_1 pA^{-1}b_0(s_1)]}{(s - s_1)^2 (p - j\omega/U)} ds_1, \end{aligned} \tag{70}$$

$$\begin{aligned} \tilde{\mu}_2(s, p; A) &= -\frac{1}{8}c^2 \tilde{H}(cpA^{-1}) \\ &\quad \times \int_{-1}^1 \frac{c_1 \tilde{G}(p|s - s_1|) [\tilde{H}(c_1 pA^{-1})(b_0(s_1) + b_1(s_1)) + \frac{1}{2}c_1 pA^{-1}b_0(s_1)]}{(s - s_1)^2 (p - j\omega/U)} ds_1. \end{aligned} \tag{71}$$

When inverting the above expressions the pole at  $p = j\omega/U$  gives the steady-state oscillatory lift and moment. Before writing down the results, we define a number of terms, to appear in the final expressions: reduced frequency based on the semichord

$$\sigma = \omega c A^{-1} / U,$$

reduced frequency based on the span length  $|s - s_1|$

$$\eta = \omega |s - s_1| / U,$$

Theodorsen's function

$$\left. \begin{aligned} \Theta(\sigma) &= \tilde{H}(j\sigma) = K_1(j\sigma) / [K_0(j\sigma) + K_1(j\sigma)], \\ \Pi(\eta) &= \tilde{G}(j\eta) = \frac{1}{2} \pi j \eta [\mathbf{H}_1(j\eta) - Y_1(j\eta) - 2/\pi], \\ \Omega(\sigma) &= \Theta(\sigma) + \frac{1}{2} j\sigma. \end{aligned} \right\} \tag{72}$$

The steady-state results can now be found by inspection of (68)–(71).

$$\left. \begin{aligned}
 l(s, t; A) &= -\frac{\pi\rho U c}{A} \left\{ b_0(s) \Omega(\sigma) + b_1(s) \Theta(\sigma) \right. \\
 &\quad \left. + \frac{\Omega(\sigma)}{2A} \int_{-1}^1 \frac{c_1 \Pi(\eta)}{(s-s_1)^2} [b_0(s_1) \Omega(\sigma_1) + b_1(s_1) \Theta(\sigma_1)] ds_1 \right\} \exp(j\omega t), \\
 m(s, t; A) &= -\frac{\pi\rho U c^2}{2A^2} \left\{ b_1(s) (1 + \frac{1}{4}j\sigma) - [b_0(s) + b_1(s)] \Theta(\sigma) \right. \\
 &\quad \left. - \frac{\Theta(\sigma)}{2A} \int_{-1}^1 \frac{c_1 \Pi(\eta)}{(s-s_1)^2} [b_0(s_1) \Omega(\sigma_1) + b_1(s_1) \Theta(\sigma_1)] ds_1 \right\} \exp(j\omega t), \\
 &\quad \sigma_1 = \omega c_1 A^{-1} / U \quad (c_1 = c(s_1)).
 \end{aligned} \right\} \quad (73)$$

For physical interpretation, the real part of these equations must be taken. The quantities  $\Theta$ ,  $\Pi$  and  $\Omega$  are complex. Their real and imaginary parts are plotted in figures 2(a) and (b). The appendix presents these functions explicitly, together with their asymptotic forms for large and small values of their arguments. The steady-state results for a wing at constant incidence  $-\alpha$  to an impulsively generated uniform stream  $U$  (see (60)) become a special case of (73), on setting  $\omega = 0$ ,  $b_1 = 0$  and  $b_0 = -2U\alpha$ .

For high-frequency oscillations (say,  $\omega \sim O(A)$ ),

$$\Omega(\sigma) \sim \frac{1}{2}j\sigma + O(1), \quad \Theta(\sigma) \sim \frac{1}{2} + O(\sigma^{-1}) \quad \text{and} \quad \Pi(\eta) \sim -j/\eta + O(\eta^{-3}).$$

If we define the ratios of the three-dimensional correction term to the two-dimensional lift and moment as  $\epsilon$  and  $\delta$ , respectively, then

$$\epsilon = \frac{1}{4}cA^{-2} \int_{-1}^1 \frac{c_1}{|s-s_1|^3} \frac{|b_0(s_1) \Omega(\sigma_1) + b_1(s_1) \Theta(\sigma_1)|}{|b_0(s) \Omega(\sigma) + b_1(s) \Theta(\sigma)|} ds_1,$$

$$\text{and} \quad \delta = \frac{1}{4}U/\omega A^{-1} \int_{-1}^1 \frac{c_1}{|s-s_1|^3} \frac{|jb_0(s_1) \Omega(\sigma_1) + b_1(s_1) \Theta(\sigma_1)j|}{|b_1(s) (1 + \frac{1}{4}j\sigma) - (b_0(s) + b_1(s)) \Theta(\sigma)|} ds_1.$$

The integrands are clearly  $O(1)$ , so that  $\epsilon \sim O(A^{-2})$  and  $\delta \sim O(A^{-1}\omega^{-1})$ , for  $\omega > O(A)$ . Consequently, for high-frequency motion, the three-dimensional correction diminishes. For steady flow past a wing at incidence, the downwash is known to give rise to an effective angle of attack which is less than the geometric angle. For oscillatory transverse motions, the variations of the streamwise component of vorticity in the free-stream direction reduce the adverse effect of the downwash. We see that, for high-frequency oscillations, the wing acts essentially as if it has an infinite aspect ratio.

#### 4.4. Flapping wing

When the wing planform executes a lateral displacement

$$\hat{y} = \frac{1}{2}\xi_0(s) \exp(j\omega t A^{-1}) \quad (|\hat{x}| \leq c, |s| \leq 1),$$

we have a case of flapping flight. When  $\xi_0(s)$  is constant along the span, the wing oscillates in pure heave. For these cases, we have

$$l(s, t; A) \sim -\pi\rho U^2 \sigma j \xi_0(s) \Omega(\sigma) \Sigma(s) \exp(j\omega t) A^{-1}, \quad (74)$$

$$m(s, t; A) \sim \pi\rho U^2 \sigma j \xi_0(s) c A^{-1} \Theta(\sigma) \Sigma(s) \exp(j\omega t) A^{-1}, \quad (75)$$

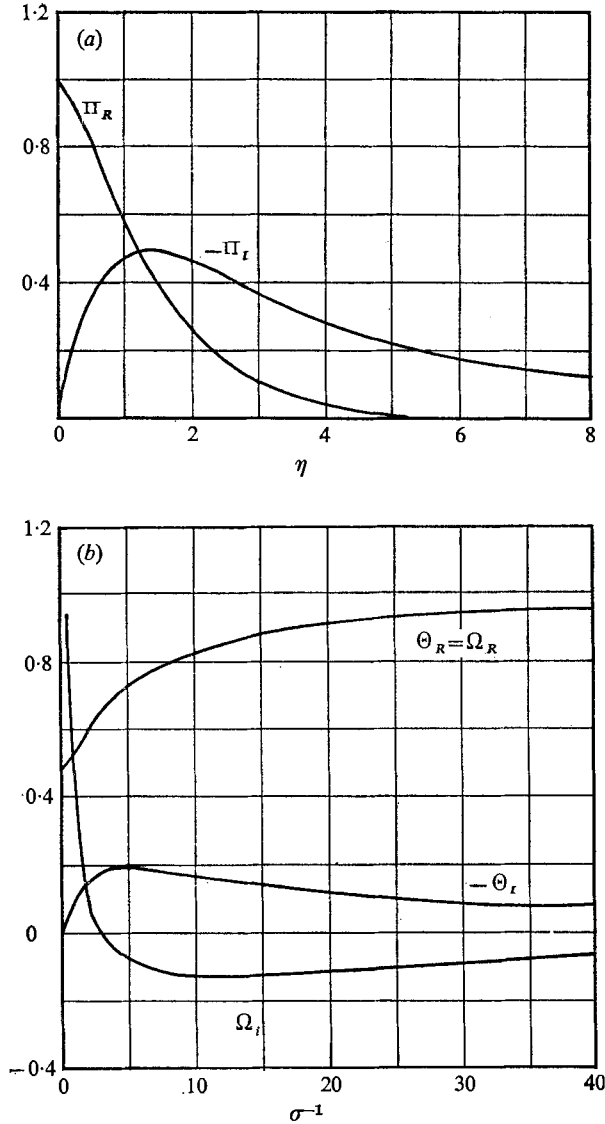


FIGURE 2. (a) Variation of real and imaginary parts of  $\Pi$ , as a function of  $\eta = (\omega/U) |s - s_1|$ . (b) Variation of real and imaginary parts of  $\Omega$  and  $\Theta$ , as a function of the inverse reduced frequency  $\sigma^{-1} = U/\omega c$ .

where 
$$\Sigma(s) = 1 + \frac{1}{2A} \int_{-1}^1 \frac{c_1 \Pi(\eta) \Omega(\sigma_1) \xi_0(s_1)}{(s - s_1)^2 \xi_0(s)} ds_1. \tag{76}$$

For flapping flight the chordwise location of the centre of pressure  $x_{cp}(s)$  is seen to depend on the reduced frequency:

$$\left. \begin{aligned} x_{cr}(s) &= -\frac{1}{2} c A^{-1} \operatorname{Re} \left[ \frac{\Theta(\sigma)}{\Omega(\sigma)} \right] = -c A^{-1} \left\{ 1 - \frac{\frac{1}{2} \sigma (\Theta_I(c) + \frac{1}{2} \sigma)}{\Theta_R^2(\sigma) + [\Theta_I(\sigma) + \frac{1}{2} \sigma]^2} \right\} \\ &\sim -\frac{1}{2} c A^{-1} \left\{ 1 + \frac{1}{4} \sigma^2 [\log(2/\gamma_1 \sigma)] \right\} \quad (\sigma \ll 1, \gamma_1 = 1.781\dots) \\ &\sim -\frac{3}{8} c A^{-1} / \sigma^2 [1 + O(\sigma^3)] \quad (\sigma \gg 1). \end{aligned} \right\} \tag{77}$$



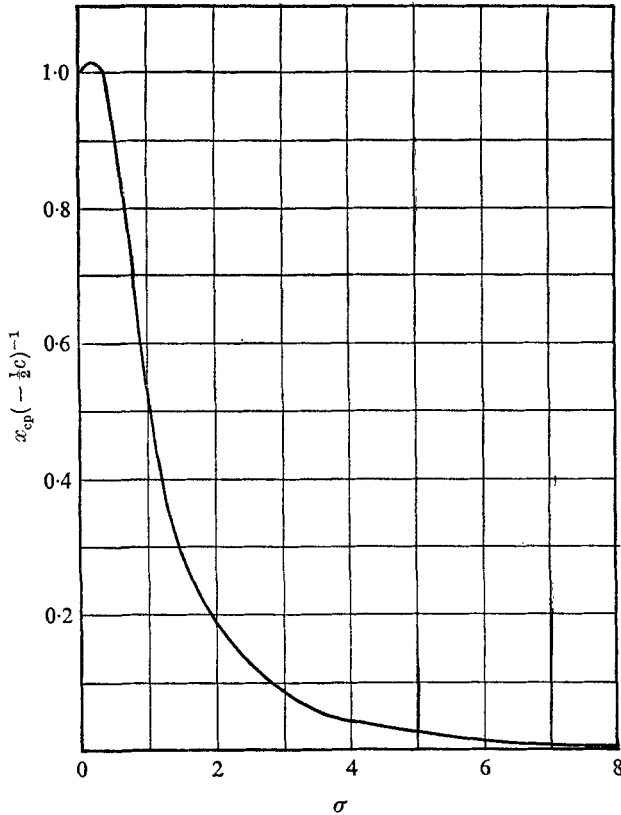


FIGURE 3. Migration of the centre of pressure, as a function of reduced frequency, for flapping flight. ( $x_{cp}(-\frac{1}{2}c)^{-1} = \text{Re}[\Theta(\sigma)/\Omega(\sigma)]$  against  $\sigma = \omega c/U$ .)

The asymptotic results indicate that the centre of pressure migrates away from the quarter-chord toward the midchord with increase of reduced frequency. The full variation of the centre of pressure is presented in figure 3.

## 5. Concluding remarks

The results of this work have been presented as asymptotic series in the inverse aspect ratio, in which three-dimensionality enters as a correction to the two-dimensional results. Besides the interesting cases of impulsive acceleration to a constant speed, constant acceleration, and simple harmonic pitching and heaving motion at constant forward speed, presented here, the theory is sufficiently general to permit quantitative treatment of a wealth of other practically important unsteady wing motions. Provided compressible effects and low Reynolds number effects remain negligible, any positive speed of advance  $U(t)$  can be entertained, as well as arbitrary 'but small' unsteady motions transverse to the wing planform.

The matching procedure renders the inner and outer expansions uniformly valid (except near certain wing tips) to one order higher in inverse aspect ratio than

the strip-theory result. It is, therefore, possible to obtain the three-dimensional effects on thrust, rate of energy loss due to vortex shedding, and the power input necessary to sustain the motion. These can be readily calculated in the near field, using the appropriate expressions for the acceleration potential, normal wing velocity, and wing displacement gradients.

The short-time solutions for lift and moment, and the high-frequency harmonic motion solutions, indicate that three-dimensional effects are not important, since they are  $O(A^{-2})$ , compared with the primary effect. For such cases, a strip theory based on two-dimensional unsteady wing section analysis can be used with confidence. However, for long-time or steady-state conditions, where accelerations are not too 'large', the three-dimensional correction is seen to be  $O(A^{-1})$ , compared with the primary effect.

The assumption that physical quantities exhibit mild spanwise variations is violated locally near the wing tips for certain tip shapes, and gives rise to a region of non-uniformity there, which becomes larger as the tip becomes blunter. For rectangular planforms, the spanwise distributions of lift and moment cannot be integrated to give total values, owing to the severity of the tip singularity. For elliptical planforms and finer shapes, the theory yields convergent total-value results.

A numerical investigation is being prepared, to assess the three-dimensional effects of pitching, rolling, heaving, flapping and coupled modes of motion, for a family of planforms, and over a range of reduced frequencies. To assess the accuracy and range of applicability of the foregoing theory, there is also need for extensive experiments.

The theory will be useful for optimization studies (Wu 1971*b*), to determine optimal wing shapes and motions under various isoperimetric conditions.

I should like to express my appreciation to the referees of this paper, for their many useful suggestions. The work reported here was sponsored by the in-house, independent exploratory development program of the Naval Ship Research and Development Center, Bethesda, Maryland 20084. It was presented at the Thirteenth International Congress of Theoretical and Applied Mechanics, August 1972, Moscow State University, U.S.S.R.

### Appendix. Real and imaginary components of $\Pi$ , $\Theta$ and $\Omega$

The complex functions  $\Pi(\eta)$ ,  $\Theta(\sigma)$  and  $\Omega(\sigma)$ , defined by (72), can be separated into their real and imaginary parts. Using Abramowitz & Stegun (1964, p. 358, (9.1.3), (9.1.4); p. 375, (9.6.4), (9.6.5); p. 498, (12.2.1)), we find that  $\Pi$ ,  $\Theta$  and  $\Omega$  can be expressed in terms of tabulated functions.

$$\begin{aligned}\Pi(\eta) &= \Pi_R(\eta) + j\Pi_I(\eta), \\ \Pi_R(\eta) &= \eta K_1(\eta), \\ \Pi_I(\eta) &= 2\eta[I_1(\eta) - \mathbf{L}_1(\eta)]/\pi - \eta, \\ \Theta(\sigma) &= \Theta_R(\sigma) + j\Theta_I(\sigma),\end{aligned}$$

$$\begin{aligned}\Theta_R(\sigma) &= [J_1^2(\sigma) + Y_1^2(\sigma) + 2/\pi\sigma][(J_1 + Y_0)^2 + (J_0 - Y_1)^2]^{-1}, \\ \Theta_I(\sigma) &= -[J_0(\sigma)J_1(\sigma) + Y_0(\sigma)Y_1(\sigma)][(J_1 + Y_0)^2 + (J_0 - Y_1)^2]^{-1}, \\ \Omega(\sigma) &= \Theta_R(\sigma) + j[\Theta_I(\sigma) + \frac{1}{2}\sigma],\end{aligned}$$

where  $L_1(\eta)$  is modified Struve function,  $J_n(\sigma)$ ,  $Y_n(\sigma)$  are Bessel functions of the first and second kinds, and  $I_1(\eta)$ ,  $K_1(\eta)$  are modified Bessel functions of the first and second kinds. The asymptotic forms of these functions, for  $\eta \ll 1$  and  $\sigma \ll 1$ , are

$$\begin{aligned}\Pi_R(\eta) &\sim 1 + \eta^2[\frac{1}{2}\log(\frac{1}{2}\eta) + \frac{1}{4}(2\gamma_1 - 1)] + O(\eta^4 \log^2 \eta), \\ \Pi_I(\eta) &\sim -\eta + \frac{1}{4}\pi\eta^2 + \frac{1}{32}\pi\eta^4 + O(\eta^5), \\ \Theta_R(\sigma) = \Omega_R(\sigma) &\sim 1 - \frac{1}{2}\pi\sigma - \sigma^2[\log^2(2/\gamma_1\sigma) - \frac{1}{4}\pi^2] + O(\sigma^3 \log^2 \sigma), \\ \Theta_I(\sigma) = \Omega_I(\sigma) - \frac{1}{2}\sigma &\sim -\sigma(1 - \pi\sigma)\log(2/\gamma_1\sigma) + O(\sigma^3 \log^3 \sigma).\end{aligned}$$

For  $\eta \gg 1$  and  $\sigma \gg 1$ ,

$$\begin{aligned}\Pi_R(\eta) &\sim (2\pi\eta)^{\frac{1}{2}}\exp(-\eta)[1 + \frac{3}{8}\eta^{-1} + O(\eta^{-2})], \\ \Pi_I(\eta) &\sim -1/\eta - 3/\eta^3 + O(\eta^{-5}), \\ \Theta_R(\sigma) = \Omega_R(\sigma) &\sim \frac{1}{2}[1 + \frac{1}{8}\sigma^2 + O(\sigma^{-4})], \\ \Theta_I(\sigma) = \Omega_I(\sigma) - \frac{1}{2}\sigma &\sim -\frac{1}{8}\sigma[1 - \frac{1}{128}\sigma^{-2} + O(\sigma^{-4})].\end{aligned}$$

The real and imaginary parts of  $\Pi$ ,  $\Theta$  and  $\Omega$  are plotted in figures 2(a) and (b).

#### REFERENCES

- ABRAMOWITZ, M. & STEGUN, I. A. 1964 *Handbook of Mathematical Functions*. U.S. National Bureau of Standards.
- ASHLEY, H. & LANDAHL, M. 1965 *Aerodynamics of Wings and Bodies*. Addison-Wesley.
- ERDÉLYI, A., MAGNUS, W., OBERHETTINGER, F. & TRICOMI, F. G. (ed.) 1954 *Tables of Integral Transforms. Bateman Manuscript Project*, vol. 1. McGraw-Hill.
- MANGLER, K. W. 1951 Improper integrals in theoretical aerodynamics. *Royal Aircraft Establishment Rep. Aero.* no. 2424.
- JAMES, E. C. 1973 A linearized theory for a wing in curved flight. *Naval Ship R. & D. Centre Rep.* no. 4098.
- VAN DYKE, M. D. 1963 Lifting-line theory as a singular-perturbation problem. *Stanford University, Department of Aeronautics, SUDAER* 165.
- VAN DYKE, M. D. 1964 *Perturbation Methods in Fluid Mechanics*. Academic.
- WU, T. Y. 1971a Hydromechanics of swimming propulsion. Part 1. Swimming of a two-dimensional flexible plate at variable forward speeds in an inviscid fluid. *J. Fluid Mech.* **46**, 337.
- WU, T. Y. 1971b Hydromechanics of swimming propulsion. Part 2. Some optimum-shape problems. *J. Fluid Mech.* **46**, 521.